High surface area titanium phosphonate materials with hierarchical porosity for multi-phase adsorption†

Tian-Yi Ma, Xiu-Zhen Lin, Xue-Jun Zhang and Zhong-Yong Yuan*

Received (in Victoria, Australia) 18th December 2009, Accepted 26th January 2010
First published as an Advance Article on the web 3rd March 2010
DOI: 10.1039/b9nj00775j

Inorganic–organic hybrid titanium phosphonate materials with a hierarchically-porous structure were synthesized by a mild solvent evaporation strategy using 1-hydroxyethylidene-1,1-diphosphonic acid as an organophosphorus coupling molecule. The preparations were accomplished with the use of triblock copolymers F127 and P123 as structure-directing agents. All the samples possessed a macroporous morphology of the mesoporous framework with a high surface area, and were characterized by SEM, TEM and N_2 sorption analysis. The hydroxyethylidene-bridged organophosphonate groups were homogeneously incorporated into the network of the hierarchical porous solid, as revealed by FT-IR, MAS NMR, TGA-DSC and XPS measurements. The hybrid materials were used as adsorbents for the liquid phase adsorption of Cu^{2+} ions in water and the gas phase adsorption of CO_2, showing high adsorption capacity and good reusability, which makes them promising adsorbents for practical applications in environmental remediation.

Introduction

As one of the most important applications of porous materials, adsorption has attracted tremendous research interest, and a large number of adsorbents have been put into practice.[1–3] An effective adsorbent should fit the qualification of multi-functionality for various adsorbates in different phases, such as liquid and gas phase adsorption, and recyclability. Heavy metal ion adsorption, especially mercury and lead, which are highly toxic environmental pollutants, is typical of liquid phase adsorption applications. Conventional methods, such as precipitation and membrane processes, are usually unfavourable, especially when dealing with large volumes of water containing metal ions in low concentration. For example, after precipitation and following filtration, the concentration of metal ions remains at the level of a few mg L^{-1}, and a great amount of waste precipitate is produced.[4] Ion exchange or adsorption with commercial activated carbon is expensive, and high costs could limit their use. Efforts have therefore been focused on low cost adsorption materials in the past ten years.[5] A series of silica-based mesoporous organic–inorganic hybrid materials have recently been developed for the removal of heavy metal ions from waste streams,[6,7] where the organic functionalities in these adsorbents typically serve to form complexes with heavy metal ions through acid–base reactions, and the solid support allows easy removal of the loaded adsorbent from the liquid waste.[8] Thiols, thiourea and amines have been used as metal ion binding motifs for the efficient removal of toxic heavy metals like Hg(II), Cu(II) and Cd(II).[6–9] Gas storage, such as H_2 sorption and CO_2 capture, is representative of gas phase adsorption. With increasing CO_2, an undesirable consequence for the Earth's environment is caused by the alteration of the temperature of the atmosphere and the acidity of the oceans. The capturing of CO_2 and its storage may play a very important role in decreasing its emission to the atmosphere. Several alternative concepts for CO_2 capture have been proposed, including chemisorption on oxide surfaces,[10] physical adsorption on porous silicates[11] and activated carbons,[12] and metal–organic framework compounds.[13] Many amine-functionalized mesoporous materials[11,14] have proved to be efficient inorganic–organic hybrid adsorbents for CO_2 through the formation of carbamate species under dry conditions between the solid amine-based adsorbent and the gaseous CO_2.[15]

However, to the best of our knowledge, there are few reports about utilizing hierarchical meso-/macroporous hybrid materials as adsorbents for heavy metal ions and CO_2, though materials with hierarchical pores have enhanced properties compared to single-sized pore materials due to increased mass transport through the large pore channels of the material and the maintenance of a specific surface area on the level of fine pore systems. Our recent work has been focused on the rational synthesis and application exploration of nanoporous phosphonate titania[16,17] and titanium phosphonate[18–20] hybrid materials, which have proved to be excellent photocatalysts under UV or visible light irradiation and also efficient adsorbents of heavy metal ions. A kind of hierarchical porous aluminium phosphonate has also been used as a multi-functional adsorbent for both heavy metal ions and proteins.[21] Nevertheless, these phosphonate hybrids were synthesized by an autoclaved aging process with relatively limited surface areas (mainly around 20–200 m^2 g^{-1}), possibly due to the existence of

Institute of New Catalytic Materials Science, Key Laboratory of Energy-Material Chemistry (Tianjin) and Engineering Research Center of Energy Storage and Conversion (Ministry of Education), College of Chemistry, Nankai University, Tianjin 300071, P. R. China. E-mail: zyyuan@nankai.edu.cn; Fax: +86 22 23509610; Tel: +86 22 23509610

† Electronic supplementary information (ESI) available: XRD patterns, FT-IR and MAS NMR spectra, and TG-DSC analysis of the synthesized hierarchical meso-/macroporous titanium phosphonate materials. See DOI: 10.1039/b9nj00775j

organic groups in the pores and surfaces.[18–20] The homogeneous incorporation of organophosphonate units into hierarchically-nanoporous metal oxide networks is still a challenge for their practical applications. Herein, we report alternative titanium phosphonate (TPPH) hybrids with hierarchically meso-/macroporous structures and high surface areas ($>370\ m^2\ g^{-1}$) by the utilization of a mild solvent evaporation strategy, in which the copolymers F127 and P123 were used as structure-directing agents and 1-hydroxyethylidene-1,1-diphosphonic acid (HEDP) was used as the coupling organophosphate molecule. Hydroxyethylidene groups were anchored in the network of the synthesized titanium phosphonates, and proved to be low-cost and efficient adsorbents of heavy metal ions and CO_2 with a good reusability.

Experimental section

Synthesis

All chemicals were used as received without further purification. In a typical synthesis procedure, 0.005 mol of 1-hydroxyethylidene-1,1-diphosphonic acid (HEDP, donated by the Henan Qingyuan Chemical Co.) was added to 50 mL of ethanol in the presence of 3 g of F127 ($EO_{106}PO_{70}EO_{106}$, Nanjing Well Chemical Corp., Ltd.) or P123 ($EO_{20}PO_{70}EO_{20}$, Nanjing Well Chemical Corp., Ltd.) with stirring, followed by the dropwise addition of 0.005 mol of tetrabutyl titanate (Kermel, A.R.). After further stirring for 24 h, the mixture was transferred into Petri dishes to evaporate the ethanol under a controlled relative humidity at 40 °C in air for 2 d. Removal of the surfactant was achieved by extraction with ethanol for 96 h. The F127 and P123 synthesized samples were marked as TPPH-F127 and TPPH-P123, respectively.

Characterization

Scanning electron microscopy (SEM) and transmission electron microscopy (TEM) were carried out on a Shimadzu SS-550 microscope at 15 keV and a Philips Tecnai G20 at 200 kV, respectively. N_2 adsorption–desorption isotherms were recorded on a Quantachrome NOVA 2000e sorption analyzer at liquid N_2 temperature (77 K). The samples were de-gassed at 150 °C overnight prior to measurements. The surface area was obtained by the 10-point Brunauer–Emmett–Teller (BET) method, and the pore size distribution was calculated from the adsorption branch of the isotherm by the non-local density functional theory (NLDFT) modelling method. Fourier transform infrared (FT-IR) spectra were measured on a Bruker VECTOR 22 spectrometer by the KBr pellet technique, and the ranges of spectrograms were 4000 to 400 cm^{-1}. Diffuse reflectance UV-vis absorption spectroscopy was employed on a JASCO V-570 UV–V-NIR spectrophotometer over the wavelength range 300–900 nm using $BaSO_4$ as a reference. X-Ray diffraction (XRD) patterns were recorded on a Rigaku D/max-2500 diffractometer with Cu-K_α radiation operating at 40 kV and 100 mA. Solid-state ^{31}P and ^{13}C magic angle spinning (MAS) nuclear magnetic resonance (NMR) spectra were recorded on a Varian Unity plus-400 spectrometer. Thermogravimetry (TG) and differential scanning calorimetry (DSC) were performed using a Netzsch STA409 instrument at a heating rate of 5° min^{-1} using α-Al_2O_3 as the reference. The chemical compositions of Ti and P were analyzed by inductively-coupled plasma (ICP) emission spectroscopy on a Thermo Jarrell-Ash ICP-9000 (N + M) spectrometer, and C, N and H were analyzed on a Vario-EL elemental analyzer. X-Ray photoelectron spectroscopy (XPS) measurements were performed on a Kratos Axis Ultra DLD (delay line detector) spectrometer equipped with a monochromatic Al-K_α X-ray source (1486.6 eV). All XPS spectra were recorded using an aperture slot of 300 × 700 microns, survey spectra were recorded with a pass energy of 160 eV, and high resolution spectra with a pass energy of 40 eV.

Cu^{2+} ion adsorption

Cu^{2+} ion adsorption tests of the hybrid mesoporous materials were performed in batch mode.[16,18] 0.01 g of the adsorbent was added into 50 mL of a homoionic solution containing different concentrations (10, 20, 30, 40, 50 mg L^{-1}) of $Cu(NO_3)_2$ (pH 7.0). The mixture was stirring for 3 h, followed by centrifugation at 6000 rpm for 15 min. 20 mL of the obtained clear solution, 12 mL of ethanol and 30 mL of dicyclohexanoneoxalyldihydrazone solution (0.4 g of dicyclohexanoneoxalyldihydrazone dissolved in 50 mL of ethanol and then adjusted to 500 mL with water) were mixed to 100 mL by adding more water, and allowed to adjust with ammonia to pH 8∼9, which is the best pH value for chromogenic reactions. The volume of Cu(II) adsorbed was monitored by measuring the UV absorption of the initial and final solutions at λ_{max} = 600 nm. The results were also proved by atomic absorption spectroscopy (AAS) analysis. For adsorption tests at different pH values, the pH values of the metal ion solutions were determined by buffers listed as follows; pH 4 and 5: potassium hydrogen phthalate buffer, pH 6: potassium phosphate buffer, pH 7: potassium dihydrogen phosphate buffer, pH 8: boric acid–potassium chloride buffer, pH 9 and 10: sodium bicarbonate buffer. To test the reusability of the hierarchical TPPH adsorbents, the Cu^{2+} ion-loaded TPPH-P123 was treated with 1 mol L^{-1} of hydrochloric acid for 8 h to remove the heavy metal ions and then neutralized, followed by a second round of metal ion adsorption testing. The adsorbents were reused 10 times in all.

CO_2 adsorption

CO_2 adsorption was characterized by a simultaneous DSC–TGA analysis using a TA SDT Q600 instrument under ambient pressure (1.0 atm). The samples were first activated by heating to 150 °C under an N_2 flow to remove adsorbed moisture, ethanol and gases, and then cooled to 30 °C in an N_2 flow. During the sorption experiments, the samples were purged with CO_2 (20 $cm^3\ min^{-1}$). Upon introduction of the gas, a weight gain was observed due to CO_2 physical absorption on the sample surface. CO_2 uptake of the samples was also tested at 35 and 75 °C. Desorption of CO_2 was performed by purging with N_2 (100 $cm^3\ min^{-1}$) for 180 min. 33 cycles of adsorption and desorption were repeated in order to test the ability of the sorbents to retain their CO_2 sorption capacity.

Results and discussion

Adsorbent synthesis and characterization

The meso-/macroporous titanium phosphonate materials were synthesized by a mild solvent evaporation strategy method using triblock copolymers F127 and P123 as structure-directing agents. Fig. 1 shows representative SEM and TEM images of the synthesized materials. The macropores of TPPH-P123 and TPPH-F127 are channel-like in shape with a uniform pore diameter distribution of 800–1200 nm. The macrochannels are mainly of one-dimensional orientation, parallel to each other (Fig. 1a and b), which is quite similar to previously reported meso-/macroporous titanium phosphate materials.[22] The TEM images (Fig. 1c and d) reveal that the walls of the macroporous network of both TPPH-F127 and TPPH-P123 are composed of titanium phosphonate aggregates with sizes of tens of nanometers, and showing wormhole-like mesopores. By carefully comparing the TEM images of the two samples, the nanoparticles in the pore walls of TPPH-P123 were of smaller average size and tighter aggregation than those of TPPH-F127, which may be of benefit through a higher specific surface area.

Fig. 2 shows the N_2 adsorption–desorption isotherms and the corresponding pore size distribution curves of hybrids TPPH-P123 and TPPH-F127. The isotherms are of type II, showing a gradual increase of N_2 adsorbed volume with increased relative pressure. This indicates an appreciable amount of macroporosity in the synthesized samples, which is in agreement with the SEM images. The isotherms do not level off at relative pressures close to the saturation vapor pressure, making type H3 hysteresis loops, which were reported for materials comprised of aggregates (loose assemblages) of plate-like particles forming slit-like pores.[23] The pore width distribution curves estimated using the NLDFT model show one narrow peak in the range 2–3 nm (Fig. 2, right). It is notable that large surface areas of 377 and 511 $m^2\ g^{-1}$, and pore volumes of 0.51 and 0.67 $m^3\ g^{-1}$ were accessed for TPPH-F127 and TPPH-P123, respectively. The surface area of TPPH-P123 is much higher than most of the previously reported porous metal phosphonate materials,[18–20,24–25] and is comparable to some ordered mesoporous aluminium phosphonate materials (around 500 $m^2\ g^{-1}$),[26–28] which means that the surfactant-assisted solvent evaporation process is effective for obtaining hierarchical porous structures with enlarged specific surface areas in the synthesized materials. The formation mechanism of the present hierarchical meso-/macroporous structure could be related to a surfactant-induced self-assembly process.[22,29] Tetrabutyl titanate is hydrolyzed in the HEDP ethanol solution to form nanometer-sized TPPH particles and simultaneously generate many butanol molecules. Microemulsions are formed under stirring in this system containing water, butanol and surfactant (F127 or P123) micelles. The self-assembly of TPPH particles and aggregations of TPPH along with the microemulsions happens together to produce the mesostructures. Also, hydrolysis reactions and polycondensation might produce microphase-separated domains of TPPH-based nanoparticles and water/alcohol channels, which are the initiators of the macrochannels.[18,19] After solvent evaporation and the surfactant extraction process, accessible mesopores and macropores are obtained.

All of the synthesized samples possess amorphous framework walls, as revealed by wide angle powder XRD patterns (Fig. S1 in the ESI†). No crystalline $TiPO_4$ or TiO_2 phases appear. One single and broad diffraction peak is present in the low angle region (the inset in Fig. S1 in the ESI†), suggestive of the packing of regularly-sized titanium phosphonate nanoparticles,[30] giving mesovoids without long-range order. This is consistent with the TEM and N_2 adsorption analysis. In the FT-IR spectra (Fig. S2 in the ESI†) of the synthesized TPPH samples, the strong broad band at 3400 cm^{-1} and sharp band at 1638 cm^{-1} correspond to the surface-adsorbed water and hydroxyl groups. The band at 1040 cm^{-1} is due to P–O···Ti stretching vibrations.[17,20] The bands at 1380 and 1450 cm^{-1} could be attributed to phosphoryl (P═O) and P–C stretching vibrations, respectively. The band at 927 cm^{-1} in the spectrum of HEDP, assigned to P–OH stretching vibrations, was not observed in the synthesized TPPH materials, which implies the extensive condensation and coordination of the

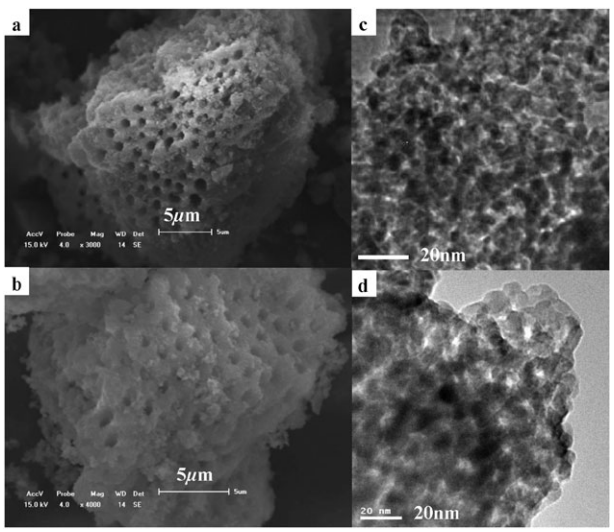

Fig. 1 SEM images of the synthesized (a) TPPH-P123 and (b) TPPH-F127, and TEM images of (c) TPPH-P123 and (d) TPPH-F127.

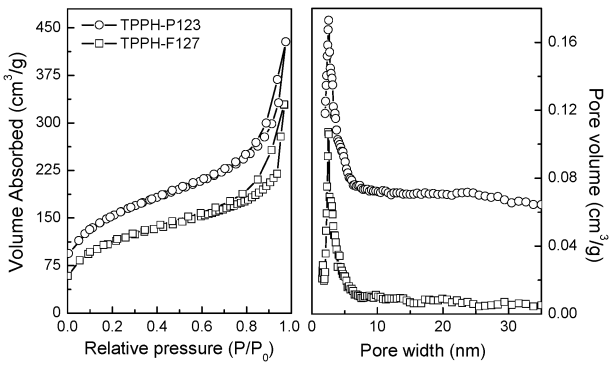

Fig. 2 N_2 adsorption–desorption isotherms (left) and pore width distribution curves determined by the NLDFT method (right) of the samples. The pore volume was shifted by 0.06 for TPPH-P123.

phosphoryl oxygen with the titanium atoms, leading mainly to bidentate phosphonate units.[17,20]

^{31}P and ^{13}C MAS NMR spectra of the resultant TPPH-F127 sample were also recorded (Fig. S3 in the ESI†) and taken as being representative. One resonance at 16.6 ppm was observed in ^{31}P NMR spectrum, which can be attributed to diphosphonate groups (≡P–C(OH)(CH_3)–P≡) linked to the Ti atoms.[26–28] The sharp ^{31}P NMR signal of a layered titanium phosphonate was not observed at −4 ppm. The ^{13}C MAS NMR spectrum of the sample exhibited resonances at 19.7 and 69.1 ppm, which correspond to the C atoms of the terminal CH_3 group and the quaternary carbon atom connected to the P═O group of the phosphonate, respectively. It was thus deduced from the FT-IR and NMR results that the organophosphonate groups were homogeneously anchored in the hierarchical porous solids.

The amount of water and the thermal stability of the synthesized TPPH-P123 material were determined by thermal gravimetric analysis (TGA) and differential scanning calorimetry (DSC). The TGA curve (Fig. S4 in the ESI†) demonstrates an initial weight loss of 11.62% from room temperature to 226 °C, accompanied by an endothermal peak at around 110 °C in the DSC curve, which may be assigned to the desorption of the adsorbed and intercalated water. The weight loss of 7.12% from 226 to 650 °C, accompanied by two exothermic peaks at 306 and 555 °C, can be attributed to the decomposition of the organic species and coke combustion. Thus, 1.7 molecules of H_2O per formula unit were calculated. Together with the elemental analysis results, a molecular unit of Ti($O_3PC(CH_3)(OH)PO_3$)·1.7H_2O can be formulated for both TPPH-F127 and TPPH-P123; an alternative formulation can be expressed as Ti(HEDP)·1.7H_2O.

High-resolution XPS spectra were also acquired on the surface of the TPPH-P123 sample to investigate its chemical state and surface stoichiometry (Fig. 3), and are taken as being representative. The Ti 2p line of TPPH-P123 is composed of two single peaks situated at 459.4 eV for Ti $2p_{3/2}$ and 465.2 eV for Ti $2p_{1/2}$, which are characteristic of Ti^{4+}. The P 2p binding energy of TPPH-P123 is observed at around 133.1 eV, characteristic of P^{5+} in phosphonate groups. No peaks of Ti–P bonds appear at 128.6 eV. The broad O 1s signals at 531.2 eV, with a shoulder at around 532.9 eV, are ascribed to the oxygen co-contributed from Ti–O, P–O and P═O bonds, respectively. The surface atomic composition of the materials was calculated to be 5.30% Ti, 10.48% P, 38.70% C and 45.52% O for TPPH-P123. The surface Ti/P ratio was calculated to be 0.48, approximately 1 : 2, suggesting a compositional homogeneity throughout the hybrid material.

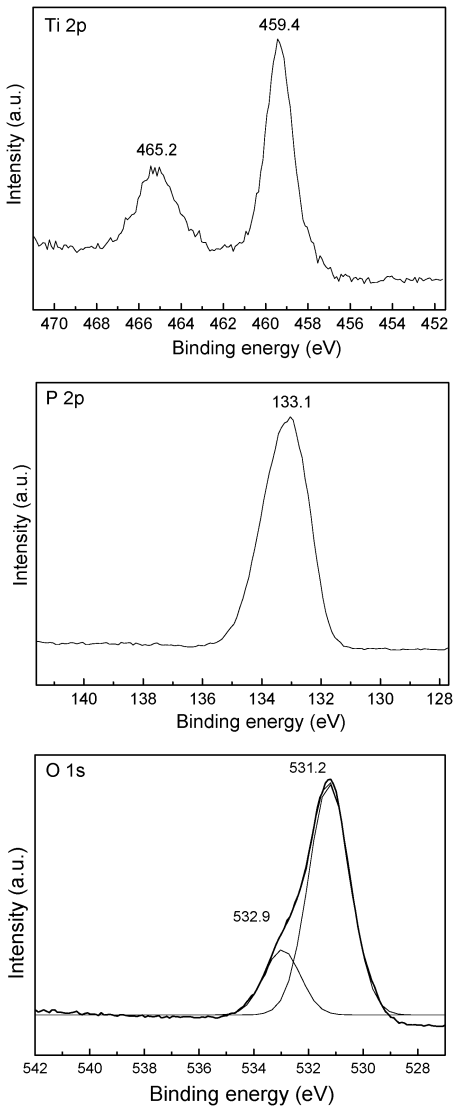

Fig. 3 High-resolution XPS spectra of the Ti 2p, P 2p and O 1s regions of TPPH-P123.

Cu^{2+} ion adsorption

Heavy metal ions, especially mercury and lead, are highly toxic environmental pollutants. The synthesized meso-/macroporous titanium phosphonate materials contain organic functional groups in the framework that could demonstrate some interaction the heavy metal ions. Thus, their performance in the adsorption of heavy metal ions, exemplified by Cu^{2+} ions, were studied. To find the optimal pH value for Cu^{2+} ion adsorption in TPPH materials, the hybrid adsorbents were tested at pH 4.0, 5.0, 6.0, 7.0, 8.0, 9.0 and 10.0, respectively (Fig. 4). The adsorption efficiency increased from pH 4.0 to 7.0, and exhibited the highest adsorption efficiency at pH = 7.0. When the pH value was further increased, the percentage of Cu^{2+} removed decreased dramatically. This is quite similar behavior to previously reported inorganic–organic hybrid adsorbents, the adsorption behaviours of which were often tested in near neutral systems.[6,9,16]

The percentage of Cu^{2+} ions removed roughly suggests the ability of the synthesized TPPH materials to adsorb Cu(II) from homoionic solutions with different concentrations at pH 7.0. When the concentration of Cu(II) was low (10–20 mg L^{-1}), most heavy metal ions in the solution could be removed, leading to a stable percentage of Cu^{2+} being removed by TPPH-F127 (10 mg L^{-1}: 94.8%, 20 mg L^{-1}: 91.7%) and by TPPH-P123 (10 mg L^{-1}: 98.1%, 20 mg L^{-1}: 96.5%). When the Cu(II) concentration was increased (30–50 mg L^{-1}), the percentage curves of Cu^{2+} removed decreased dramatically.

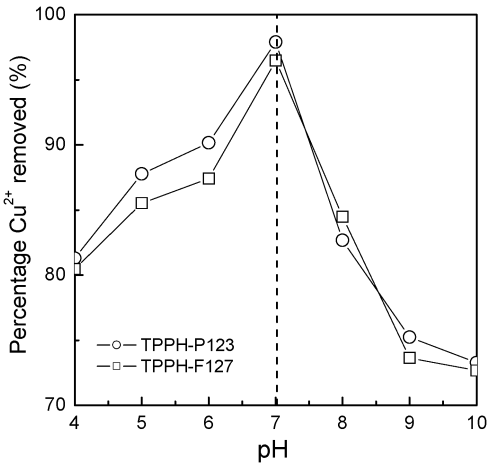

Fig. 4 The percentage Cu^{2+} removed by the synthesized TPPH materials under different pH values (treated with a 10 mg L^{-1} $Cu(NO_3)_2$ solution).

The adsorption ability of the present hybrid materials synthesized by this mild solvent evaporation method is better than our previously-reported three-dimensionally ordered macroporous titanium phosphonate adsorbents with intra-framework hydroxyethylidene groups,[20] which could remove 81.1–90.1% of the Cu^{2+} in water at low ion concentrations. The same HEDP molecule was used in these materials, and the superior adsorption ability of the present TPPH materials may be due to the well-structured porous hierarchy and higher specific surface areas of TPPH-F127 and TPPH-P123 than that of the macroporous titanium phosphonate adsorbents without mesoporosity (BET: around 25 m^2 g^{-1}). The adsorption isotherms of TPPH-P123 and TPPH-F127 are compared in Fig. 5a. The adsorption of Cu^{2+} ions by the TPPH adsorbents appeared to follow Langmuir-type behavior, with the ions being almost quantitatively adsorbed until binding saturation is reached. The maximal adsorption capacity was calculated by the Langmuir model using the equation $n_s = Kn_m c/(1 + Kc)$ where K is the Langmuir constant, c is the Cu^{2+} concentration, n_m is the monolayer adsorption capacity (maximal adsorption capacity) and n_s is the amount of Cu^{2+} adsorbed on the adsorbent. The maximal adsorption capacities were calculated as 139.4 mg g^{-1} (R^2 = 0.9972) and 136.6 mg g^{-1} (R^2 = 0.9905) for TPPH-P123 and TPPH-F127, respectively. The distribution coefficient (K_d) was determined using the equation $K_d = (c_i - c_f)V_{soln}/(c_f m_{ads})$ where c_i is the initial metal ion concentration, c_f is the ion concentration after adsorption, V_{soln} is the volume of the solution (in mL) and m_{ads} is the amount of adsorbent (in g). The distribution coefficient profiles are shown in Fig. 5b. At low concentrations of Cu(II) (10–20 mg L^{-1}), the K_d value of TPPH-F127 (92 405 mL g^{-1}) is smaller than that of TPPH-P123 (232 273 mL g^{-1}). For the previous macroporous adsorbents,[20] the K_d values were only 23 000–45 000 mL g^{-1} at low Cu^{2+} concentration, also indicating the superiority of the present TPPH-P123 and TPPH-F127 adsorbents with high surface areas. With the concentration of Cu(II) increasing to 50 mg L^{-1}, the K_d values decrease sharply to 5823 mL g^{-1} for TPPH-F127 and 6829 mL g^{-1} for TPPH-P123. This suggests that the adsorption is closely related to the concentration of the ions, and TPPH-P123 with a higher surface area is obviously a better adsorbent than TPPH-F127. Moreover, the K_d value for the TPPH-F127 and TPPH-P123 adsorbents are comparable to those of Cu(II) adsorbents made up of functionalized mesoporous silica,[8,9] indicating that the TPPH adsorbents are equally useful for removing metal ions, such as Cu(II), from water. It is also supposed that the present hierarchical titanium phosphonate adsorbents could be efficient at removing other kinds of heavy metal ions from water, including Pb^{2+}, Cd^{2+} and Hg^{2+}.

To test the reusability of the hierarchical TPPH adsorbents, a Cu^{2+} ion loaded TPPH-P123 sample, taken as representative, was treated with 1 mol L^{-1} hydrochloric acid for 8 h to remove the heavy metal ions and then neutralized, followed by a second round of metal ion adsorption testing. The results for Cu^{2+} ion adsorption using the regenerated adsorbents are summarized in Fig. 6. Only a small decrease (0.64%) in the adsorption efficiency was seen during the second use, and the sample retained Cu^{2+} an uptake capacity of 96.45% after four cycles. The Cu^{2+} uptake capacity decreased gradually with further successive use, but the material still retained greater than 70% of its original metal ion loading capacity after ten cycles. After hydrochloric acid treatment, a few Cu^{2+} ions could be retained and so occupy the coordination sites for further adsorption or even transform into $CuO/Cu(OH)_2$,

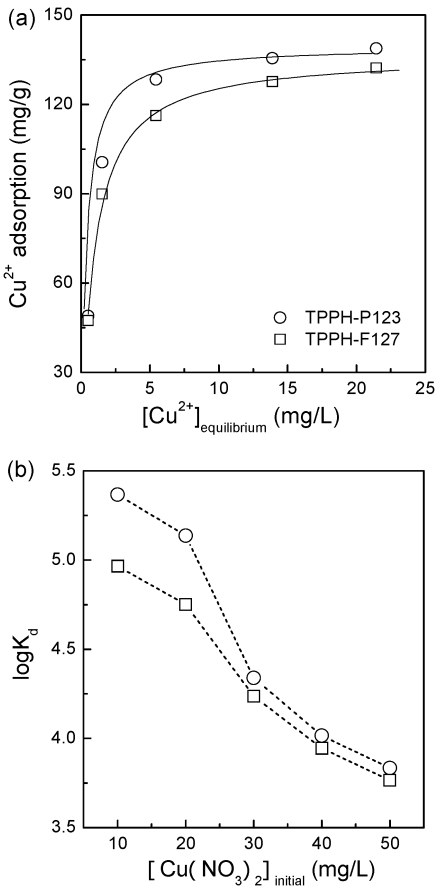

Fig. 5 (a) Cu^{2+} adsorption isotherms and (b) log K_d curves of the synthesized hybrid adsorbents.

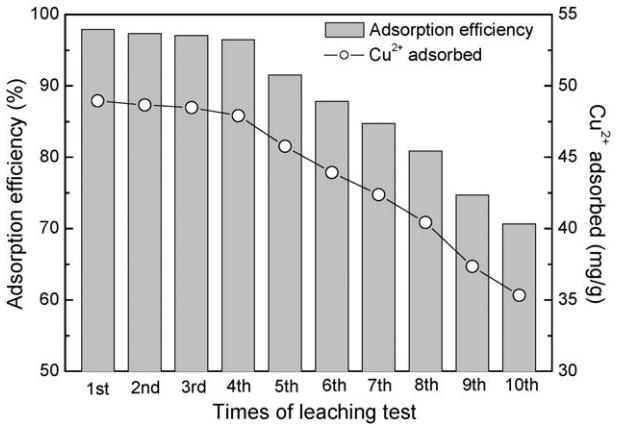

Fig. 6 Reusability of the adsorbent TPPH-P123 for Cu^{2+} (10 mg L^{-1}).

bulk blocking the pore channels. The superposition of these effects after many cycles would finally lead to a decrease of adsorption capacity. In summary, the reusability test suggests the stability of the synthesized hierarchical titanium organophosphonate materials and the retention of their adsorption properties under relatively strong acid leaching conditions, making them useful as reusable sorbents for multiple metal ion adsorption cycles.

The observed high adsorption ability of inorganic–organic hybrid titanium phosphonates is mainly caused by the bridged phosphonates containing ligands for binding metal ions, including the OH connected to the methylene and P–O of HEDP.[20] These two different binding modes are represented in the FT-IR spectrum of Cu-TPPH-P123 (TPPH-P123 loaded Cu^{2+}) (Fig. 7a). The spectrum reveals P–C stretching vibrations at 1463 cm^{-1} and a P–O···Ti stretching mode at 1010 cm^{-1}, which shows a slight shift compared to the unloaded TPPH-P123: +13 cm^{-1} and −30 cm^{-1}, respectively. Moreover, Cu-TPPH-P123 was characterized by UV-vis diffuse-reflectance spectroscopy (Fig. 7b). A sharp fall of absorbance between 300 and 350 nm can be seen in Cu-TPPH-P123, while a broad shoulder appears, ranging from 600 to 900 nm. The phenomenon is also related to the Cu complex on the surface of the material,[6] and titanium phosphonate framework plays the most important role in providing coordination sites. There have been reports about hierarchical porous materials as catalysts and adsorbents,[17,22,31,32] in which the advantages of both macropores and mesopores are demonstrated. In the present work, the reduced resistance to diffusion and the improved mass transfer could be caused by macropores or macrochannels, as well as the establishment of an adsorption/desorption equilibrium, benefiting the adsorption efficiency of the hybrid adsorbents. The well-defined mesopores and high surface areas mainly contribute to supplying accessible intra-framework bonding sites, allowing coordination between heavy metal ions and the hybrid framework. Our previously reported 3D macroporous titanium phosphonate materials, which were prepared by the same phosphonic acid HEDP,[20] exhibited a lower adsorption capacity due only to the absence of mesoporosity and low surface area.

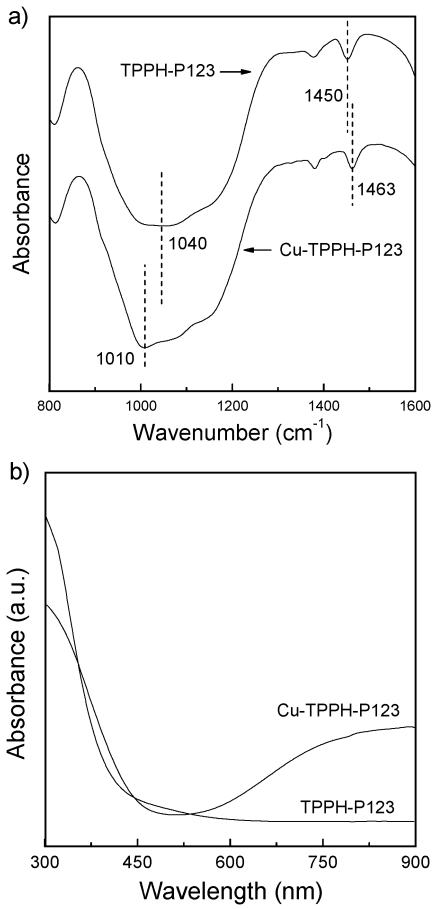

Fig. 7 (a) FT-IR and (b) UV-vis diffuse-reflectance spectra of TPPH-P123 and Cu-TPPH-P123.

CO_2 adsorption

CO_2 has drawn particular attention for being one of the major greenhouse gases contributing to global warming. To reduce the emission of CO_2, high-capacity CO_2-selective adsorbents like activated carbon,[33] zeolite[34] and mesoporous silica materials surface-modified by different types of amines,[11,14] have been widely studied. Hence, it is interesting to estimate the CO_2 adsorption performance of hierarchical porous titanium phosphonate materials. The adsorption was performed at ambient temperature and pressure to meet the broad needs of industry and households. Fig. 8 illustrates the CO_2 adsorption of TPPH-P123 and TPPH-F127 samples at 35 and 75 °C, respectively. The CO_2 adsorption capacity increased slowly and took a long time to reach equilibrium, different to the results reported in the literature, where CO_2 uptake was initially quite rapid and then began to slow after a couple of minutes, with an apparent equilibrium soon being established on the silica matrix modified by amine.[35] The difference indicates that the CO_2 adsorption on TPPH samples is physical adsorption and that CO_2 and N_2 are adsorbed together. However, when the samples are purged with CO_2, N_2 is slowly exchanged for CO_2. Therefore the equilibrium is only slowly established. The CO_2 uptake was 0.75 mmol g^{-1} for TPPH-P123 and 0.63 mmol g^{-1} for TPPH-F127 after 100 min of flow purging with CO_2 at 35 °C, which is higher than some pure

silica adsorbents (0.52 mmol g^{-1} at 20 °C) reported by Chaffee *et al.*,[36] with specific surface areas up to 909 m^2 g^{-1}. The TPPH hybrid materials have higher CO_2 capacities than pure silica materials, with larger specific surface areas, which indicates that there must be much stronger van der Waals forces between the as-synthesized materials and CO_2, resulting from the existence of phosphonate groups in the inorganic–organic network, which of course are not present in pure silica materials. For physical adsorption, gas uptake is related to morphological properties such as specific surface area, the micro-architecture of the material and the interaction strength between the adsorbent and adsorbate.[35,36] Thus, it is normal that TPPH-P123, with a higher specific surface area, has a larger CO_2 adsorption capacity than TPPH-F127. In addition, the micro-morphology of macro-channels has been proved to contribute to reduced resistance to diffusion and improved mass transfer, as well as to the establishment of an adsorption/desorption equilibrium, benefiting through an improvement in adsorption efficiency of hybrid adsorbents.[21] This provides superior CO_2 uptake in hierarchical porous materials compared to bulk materials with a similar surface area and pore volume. The CO_2 uptakes were 0.49 and 0.46 mmol g^{-1} for TPPH-P123 and TPPH-F127, respectively, after 100 min of purging with CO_2 gas at 75 °C. It seems that the CO_2 uptake of each sample decreased sharply, corresponding to the physical sorption characteristic, where the adsorption uptake reduces with increasing temperature.[33,34]

Reusability is another important characteristic of a good adsorbent. Thus, the TPPH samples were tested over multiple cycles (33) of CO_2 adsorption and desorption to confirm that the adsorption capacity was retained. TPPH-P123 was used as a representative sample at 35 °C. As can be seen in Fig. 9, the adsorption capacity remained stable at around 0.75 mmol g^{-1}, even after 33 cycles. This is quite different from some reported lime-based CO_2 adsorbents,[37,38] the adsorption capacity of which decrease continuously depending on the number of cycles due to an unavoidable decay in carbonation conversion. The as-prepared hierarchical porous TPPH materials have therefore proved to be practical adsorbents at ambient temperature and pressure with a good reusability. However,

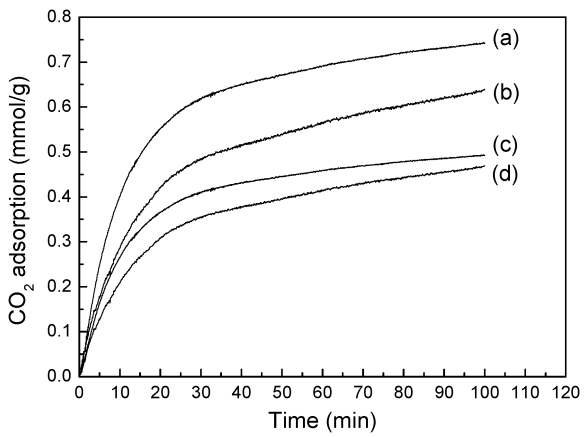

Fig. 8 TGA records of CO_2 adsorption for (a) TPPH-P123 at 35 °C, (b) TPPH-F127 at 35 °C, (c) TPPH-P123 at 75 °C and (d) TPPH-F127 at 75 °C.

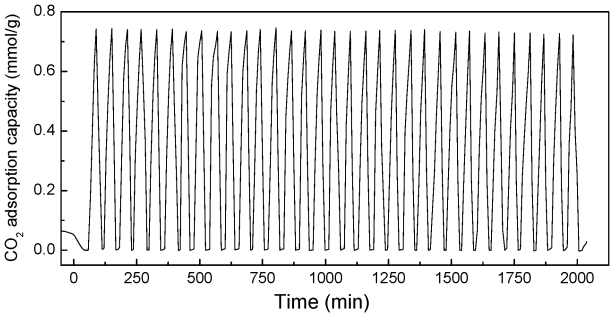

Fig. 9 Multiple cycles of CO_2 adsorption measurements for TPPH-P123.

unfortunately, the as-prepared materials do not have the same selectivity for CO_2 adsorption as some zeolites[34] and MOF[39] materials, which possess a selective adsorption capacity for CO_2 due to their pore size limits. Therefore, we are trying to synthesize a porous titanium phosphonate material with a controlled morphology and pore size to maximise the favorable interaction between the hybrid framework of metal phosphonates and CO_2 to enhance both its CO_2 uptake and selectivity. This work is now in progress.

Conclusions

High surface area titanium organophosphonate hybrid materials with a hierarchical macro-/mesoporous structure have been prepared using 1-hydroxyethylidene-1,1-diphosphonic acid as an organophosphorus coupling molecule in the presence of triblock copolymers F127 and P123. The mild solvent evaporation strategy proved to be effective in obtaining hierarchical meso-/macroporous structures with enlarged surface areas of the synthesized TPPH materials. An interesting metal ion adsorption ability was demonstrated for the synthesized materials, with the optimal pH value for Cu^{2+} ion adsorption being at pH 7.0. The adsorption of Cu^{2+} ions by the synthesized TPPH adsorbents appeared to follow Langmuir-type behaviour, with an outstanding reusability. The high adsorption capacities were comparable to other reported functionalized mesoporous silica-based adsorbents, suggesting potential in practical applications. The TPPH materials were also confirmed as useful adsorbents for CO_2 adsorption with good reusability. By utilizing this solvent evaporation strategy and using different types of phosphonic acid, the fabrication of other titanium phosphonate materials with different organic bridging groups and hierarchical nanoporous structures can also be expected to have significant efficiency in both liquid phase and gas phase adsorption.

Acknowledgements

This work was supported by the National Natural Science Foundation of China (no. 20973096 and 20673060), the National Basic Research Program of China (no. 2009CB623502), the Specialized Research Fund for the Doctoral Program of Higher Education (20070055014), the Natural Science Foundation of Tianjin (08JCZDJC21500), the MOE Supporting

Program for New Century Excellent Talents (NCET-06-0215) and Nankai University.

References

1 V. Antochshuk and M. Jaroniec, *Chem. Commun.*, 2002, 258–259.
2 S. Z. Qiao, H. Djojoputro, Q. H. Hu and G. Q. Lu, *Prog. Solid State Chem.*, 2006, **34**, 249–256.
3 A. Vinu, V. Murugesan and M. Hartmann, *J. Phys. Chem. B*, 2004, **108**, 7323–7330.
4 A. Méndez, S. Barriga, J. M. Fidalgo and G. Gascó, *J. Hazard. Mater.*, 2009, **165**, 736–743.
5 A. Méndez, G. Gascó, M. M. A. Freitas, G. Siebielec, T. Stuczynski and J. L. Figueiredo, *Chem. Eng. J.*, 2005, **108**, 169–177.
6 S. Dai, M. C. Burleigh, Y. Shin, C. C. Morrow, C. E. Barnes and Z. Xue, *Angew. Chem., Int. Ed.*, 1999, **38**, 1235–1239.
7 A. M. Liu, K. Hidajat, S. Kawi and D. Y. Zhao, *Chem. Commun.*, 2000, 1145–1146.
8 R. C. Schroden, M. Al-Daous, S. Sokolov, B. J. Melde, J. C. Lytle, A. Stein, M. C. Caubajo, J. T. Fernández and E. E. Rodríguez, *J. Mater. Chem.*, 2002, **12**, 3261–3267.
9 L. Mercier and T. J. Pinnavaia, *Environ. Sci. Technol.*, 1998, **32**, 2749–2754.
10 C. Salvador, D. Lu, E. J. Anthony and J. C. Abanades, *Chem. Eng. J.*, 2003, **96**, 187–195.
11 N. Hiyoshi, K. Yogo and T. Yashima, *Chem. Lett.*, 2004, **33**, 510–511.
12 M. Heuchel, G. M. Davies, E. Buss and N. A. Seato, *Langmuir*, 1999, **15**, 8695–8705.
13 A. R. Millward and O. M. Yaghi, *J. Am. Chem. Soc.*, 2005, **127**, 17998–17999.
14 R. Serna-Guerrero, E. Dána and A. Sayari, *Ind. Eng. Chem. Res.*, 2008, **47**, 9406–9412.
15 T. Filburn, J. J. Helble and R. A. Weiss, *Ind. Eng. Chem. Res.*, 2005, **44**, 1542.
16 X. J. Zhang, T. Y. Ma and Z. Y. Yuan, *J. Mater. Chem.*, 2008, **18**, 2003–2010.
17 X. J. Zhang, T. Y. Ma and Z. Y. Yuan, *Eur. J. Inorg. Chem.*, 2008, 2721–2726.
18 X. J. Zhang, T. Y. Ma and Z. Y. Yuan, *Chem. Lett.*, 2008, **37**, 746–747.
19 T. Y. Ma, X. J. Zhang and Z. Y. Yuan, *Microporous Mesoporous Mater.*, 2009, **123**, 234–242.
20 T. Y. Ma, X. J. Zhang, G. S. Shao, J. L. Cao and Z. Y. Yuan, *J. Phys. Chem. C*, 2008, **112**, 3090–3096.
21 T. Y. Ma, X. J. Zhang and Z. Y. Yuan, *J. Phys. Chem. C*, 2009, **113**, 12854–12862.
22 T. Z. Ren, Z. Y. Yuan, A. Azioune, J. J. Pireaux and B. L. Su, *Langmuir*, 2006, **22**, 3886–3894.
23 M. Kruk and M. Jaroniec, *Chem. Mater.*, 2001, **13**, 3169–3183.
24 M. Vasylyev and R. Neumann, *Chem. Mater.*, 2006, **18**, 2781–2783.
25 M. Vasylyev, E. J. Wachtel, R. Popovitz-Biro and R. Neumann, *Chem.–Eur. J.*, 2006, **12**, 3507–3514.
26 T. Kimura, *Chem. Mater.*, 2003, **15**, 3742–3744.
27 T. Kimura, *Chem. Mater.*, 2005, **17**, 337–344.
28 T. Kimura, *Chem. Mater.*, 2005, **17**, 5521–5528.
29 T. Z. Ren, Z. Y. Yuan and B. L. Su, *Chem. Commun.*, 2004, 2730–2731.
30 A. Vantomme, Z. Y. Yuan, G. Du and B. L. Su, *Langmuir*, 2005, **21**, 1132–1135.
31 Z. Y. Yuan and B. L. Su, *J. Mater. Chem.*, 2006, **16**, 663–677.
32 G. S. Shao, X. J. Zhang and Z. Y. Yuan, *Appl. Catal., B*, 2008, **82**, 208–218.
33 J. S. Lee, J. H. Kim, J. T. Kim, J. K. Suh, J. M. Lee and C. H. Lee, *J. Chem. Eng. Data*, 2002, **47**, 1237–1242.
34 S. Cavenati, C. A. Grande and A. E. Rodrigues, *J. Chem. Eng. Data*, 2004, **49**, 1095–1101.
35 G. P. Knowles, J. V. Graham, S. W. Delaney and A. L. Chaffee, *Fuel Process. Technol.*, 2005, **86**, 1435–1448.
36 G. P. Knowles, S. W. Delaney and A. L. Chaffee, *Ind. Eng. Chem. Res.*, 2006, **45**, 2626–2633.
37 J. C. Abanades and D. Alvarez, *Energy Fuels*, 2003, **17**, 308–315.
38 C. S. Martavaltzi and A. A. Lemonidou, *Microporous Mesoporous Mater.*, 2008, **110**, 119–127.
39 B. Wang, A. P. Côté, H. Furukawa1, M. O'Keeffe and O. M. Yaghi, *Nature*, 2008, **453**, 207–212.

